Transport in Porous Media manuscript No.
(will be inserted by the editor)

Effects of CO_2 Compressibility on CO_2 Storage in Deep Saline Aquifers

Victor Vilarrasa · Diogo Bolster · Marco Dentz · Sebastia Olivella · Jesus Carrera

Received: date / Accepted: date

Abstract The injection of supercritical CO_2 in deep saline aquifers leads to the formation of a CO_2 plume that tends to float above the formation brine. As pressure builds up, CO_2 properties, i.e. density and viscosity, can vary significantly. Current analytical solutions do not account for CO_2 compressibility. In this paper, we investigate numerically and analytically the effect of this variability on the position of the interface between the CO_2 rich phase and the formation brine. We introduce a correction to account for CO_2 compressibility (density variations) and viscosity variations in current analytical solutions. We find that the error in the interface position caused by neglecting CO_2 compressibility is relatively small when viscous forces dominate. However, it can become significant when gravity forces dominate, which is likely to occur at late times of injection.

Keywords two phase flow · CO_2 density · analytical solution · interface · gravity forces

1 Nomenclature

c_r rock compressibility
c_α compressibility of fluid α ($\alpha = c, w$)
d aquifer thickness
E_{rel} relative error of the interface position
g gravity
h_w hydraulic head of water
k intrinsic permeability

Victor Vilarrasa, Marco Dentz, Jesus Carrera
Institute of Environmental Assessment and Water Research, GHS, IDAEA, CSIC, Barcelona, Spain
Tel.: +34-93-4054169
E-mail: victor.vilarrasa@upc.edu

Victor Vilarrasa, Diogo Bolster, Sebastia Olivella
Department of Geotechnical Engineering and Geosciences, Technical, University of Catalonia (UPC), Barcelona, Spain

k_{r_α} α-phase relative permeability ($\alpha = c, w$)
N gravity number
P_{t_0} fluid pressure at the top of the aquifer prior to injection
P_{DT} fluid pressure for Dentz and Tartakovsky (2009a) approach
$\overline{P}_{DT}$ vertically averaged fluid pressure for Dentz and Tartakovsky (2009a) approach
$\overline{P}_N$ vertically averaged fluid pressure for Nordbotten et al (2005) approach
$\overline{P}_0$ vertically averaged fluid pressure prior to injection
P_α fluid pressure of α-phase ($\alpha = c, w$)
Q_m CO_2 mass flow rate
Q_0 CO_2 volumetric flow rate
$\mathbf{q}_\alpha$ volumetric flux of α-phase ($\alpha = c, w$)
R radius of influence
R_c CO_2 plume radius at the top of the aquifer for compressible CO_2
R_i CO_2 plume radius at the top of the aquifer for incompressible CO_2
r radial distance
r_0 CO_2 plume radius at the top of the aquifer
r_b CO_2 plume radius at the base of the aquifer
r_c characteristic length
r_w injection well radius
S_s specific storage coefficient
S_{r_w} residual saturation of the formation brine
S_α saturation of α-phase ($\alpha = c, w$)
t time
z vertical coordinate
z_0 depth of the top of the aquifer
z_b depth of the base of the aquifer
V CO_2 plume volume
α phase index, c CO_2 and w brine
β CO_2 compressibility
ϵ_v volumetric strain
γ_{cw} a dimensionless parameter that measures the relative importance of viscous and gravity forces
λ_α mobility of α-phase ($\alpha = c, w$)
μ_α viscosity of α-phase ($\alpha = c, w$)
ρ_0 CO_2 density at the reference pressure P_{t_0}
ρ_1 constant for the CO_2 density
$\overline{\rho}_c$ mean CO_2 density
$\overline{\rho}_{c_{DT}}$ mean CO_2 density for Dentz and Tartakovsky (2009a) approach
$\overline{\rho}_{c_N}$ mean CO_2 density for Nordbotten et al (2005) approach
ρ_α density of α-phase ($\alpha = c, w$)
σ' effective stress
ϕ porosity
ζ interface position from the bottom of the aquifer

2 Introduction

Carbon dioxide (CO_2) sequestration in deep geological formations is considered a promising mitigation solution for reducing greenhouse gas emissions to the atmosphere.

Although this technology is relatively new, wide experience is available in the field of multiphase fluid injection (e.g. the injection of CO_2 for enhanced oil recovery (Lake, 1989; Cantucci et al, 2009), production and storage of natural gas in aquifers (Dake, 1978; Katz and Lee, 1990), gravity currents (Huppert and Woods, 1995; Lyle et al, 2005) and disposal of liquid waste (Tsang et al, 2008)). Various types of geological formations can be considered for CO_2 sequestration. These include unminable coal seams, depleted oil and gas reservoirs and deep saline aquifers. The latter have received particular attention due to their high CO_2 storage capacity (Bachu and Adams, 2003). Viable saline aquifers are typically at depths greater than 800 m. Pressure and temperature conditions in such aquifers ensure that the density of CO_2 is relatively high (Hitchon et al, 1999).

Several sources of uncertainty associated with multiphase flows exist at these depths. These include those often encountered in other subsurface flows such as the impact of heterogeneity of geological media, e.g. (Neuweiller et al, 2003; Bolster et al, 2009b), variability and lack of knowledge of multiphase flow parameters (e.g. van Genuchten and Brooks-Corey models). Beyond these difficulties, the properties of supercritical CO_2, such as density and viscosity, can vary substantially (Garcia, 2003; Garcia and Pruess, 2003; Bachu, 2003) making the assumption of incompressibility questionable.

Two analytical solutions have been proposed for the position of the interface between the CO_2 rich phase and the formation brine: the Nordbotten et al (2005) solution and the Dentz and Tartakovsky (2009a) solution. Both assume an abrupt interface between phases. Both solutions neglect CO_2 dissolution into the brine, so the effect of convective cells (Ennis-King and Paterson, 2005; Hidalgo and Carrera, 2009; Riaz et al, 2006) on the front propagation is not taken into account. Each phase has constant density and viscosity. The shape of the solution by Nordbotten et al (2005) depends on the viscosity of both CO_2 and brine, while the one derived by Dentz and Tartakovsky (2009a) depends on both the density and viscosity differences between the two phases. The validity of these sharp interface solutions has been discussed in, e.g., Dentz and Tartakovsky (2009a); Lu et al (2009); Dentz and Tartakovsky (2009b).

The injection of CO_2 causes an increase in fluid pressure and displaces the formation brine laterally. This brine can migrate out of the aquifer if the aquifer is open, causing salinization of other formations such as fresh water aquifers. In contrast, if the aquifer has very low-permeability boundaries, the storage capacity will be related exclusively to rock and fluid compressibility (Zhou et al, 2008). In the latter case, fluid pressure will increase dramatically and this can lead to geomechanical damage of the caprock (Rutqvist et al, 2007). Additionally, this pressure buildup during injection gives rise to a wide range of CO_2 density values within the CO_2 plume (Figure 1). As density changes are directly related to changes in volume, the interface position will be affected by compressibility. However, neither of the current analytical solutions for the interface location acknowledge changes in CO_2 density.

The evolution of fluid pressure during CO_2 injection has been studied by several authors, e.g. (Saripalli and McGrail, 2002; Mathias et al, 2008). Mathias et al (2008) followed Nordbotten et al (2005), calculating fluid pressure averaged over the thickness of the aquifer. They considered a slight compressibility in the fluids and geological formation, but still assumed constant fluid density values. Accounting for the slight compressibility allows them to avoid the calculation of the radius of influence, which, as we propose later, can be determined by Cooper and Jacob (1946) method.

Typically CO_2 injection projects are intended to take place over several decades. This implies that the radius of the final CO_2 plume, which can be calculated with the

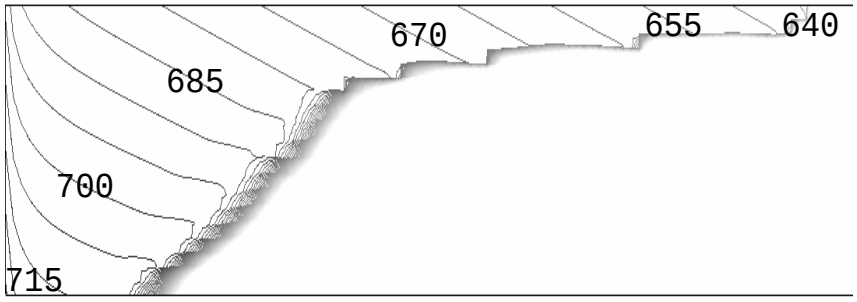

Fig. 1 CO_2 density (kg/m^3) within the CO_2 plume resulting from a numerical simulation that acknowledges CO_2 compressibility.

above analytical solutions (Stauffer et al, 2009), may reach the kilometer scale. The omission of compressibility effects can result in a significant error in these estimates. This in turn reduces the reliability of risk assessments, where even simple models can provide a lot of useful information (e.g. Tartakovsky (2007), Bolster et al (2009a)).

The nature of uncertainty in the density field is illustrated by the Sleipner Project (Korbol and Kaddour, 1995). There, around one million tones of CO_2 have been injected annually into the Utsira formation since 1996. Nooner et al (2007) found that the best fit between the gravity measurements made *in situ* and models based on time-lapse 3D seismic data corresponds to an average *in situ* CO_2 density of 530 kg/m^3, with an uncertainty of ± 65 kg/m^3. This uncertainty is significant in itself. However, prior to these measurements and calculations, the majority of the work on the site had assumed a range between 650-700 kg/m^3, which implies a significant error ($> 20\%$) in volume estimation.

Here we study the impact of CO_2 compressibility on the interface position, both numerically and analytically. We propose a simple method to account for compressibility effects (density variations) and viscosity variations and apply it to the analytical solutions of Nordbotten et al (2005) and Dentz and Tartakovsky (2009a). First, we derive an expression for the fluid pressure distribution in the aquifer from the analytical solutions. Then, we propose an iterative method to determine the interface position that accounts for compressibility. Finally, we contrast these corrections with the results of numerical simulations and conclude with a discussion on the importance of considering CO_2 compressibility in the interface position.

3 Multiphase Flow. The Role of Compressibility

Consider injection of supercritical CO_2 in a deep confined saline aquifer (see a schematic description in Figure 2). Momentum conservation is expressed using Darcy's law, which for phases CO_2, c, and brine, w, is given by

$$\mathbf{q}_\alpha = -\frac{k k_{r_\alpha}}{\mu_\alpha} \left(\nabla P_\alpha + \rho_\alpha g \nabla z \right), \quad \alpha = c, w, \tag{1}$$

where $\mathbf{q}_\alpha$ is the volumetric flux of α-phase, k is the intrinsic permeability, k_{r_α} is the α-phase relative permeability, μ_α its viscosity, P_α its pressure, ρ_α its density, g is gravity and z is the vertical coordinate.

Mass conservation of these two immiscible fluids can be expressed as Bear (1972),

$$\frac{\partial(\rho_\alpha S_\alpha \phi)}{\partial t} = -\nabla \cdot (\rho_\alpha \mathbf{q}_\alpha), \tag{2}$$

where S_α is the saturation of the α-phase, ϕ is the porosity of the porous medium and t is time.

The left-hand side of equation (2) represents the time variation of the mass of α-phase per unit volume of porous medium. Assuming that there is no external loading, and that the grains of the porous medium are incompressible, but not stationary (Bear, 1972), the expansion of the partial derivative of this term results in

$$\frac{\partial(\rho_\alpha S_\alpha \phi)}{\partial t} = S_\alpha \phi \rho_\alpha c_\alpha \frac{\partial P_\alpha}{\partial t} + \rho_\alpha S_\alpha c_r \frac{\partial P_\alpha}{\partial t} + \rho_\alpha \phi \frac{\partial S_\alpha}{\partial t}. \tag{3}$$

where $c_\alpha = (1/\rho_\alpha)(\mathrm{d}\rho_\alpha/\mathrm{d}P_\alpha)$ is fluid compressibility, $c_r = \mathrm{d}\epsilon_v/\mathrm{d}\sigma'$ is rock compressibility, ϵ_v is the volumetric strain and σ' is the effective stress.

The first term in the right-hand side of equation (3) corresponds to changes in storage caused by the compressibility of fluid phases. The second term refers to rock compressibility. The third term in the right-hand side of equation (3) represents changes in the mass of α caused by fluid saturation-desaturation processes (i.e., CO_2 plume advance). As such, it does not represent compressibility effects, although its actual value will be sensitive to pressure through the phase density, which controls the size of the CO_2 plume.

The relative importance of the first two terms depends on whether we are in the CO_2 or brine zones, because the compressibility of CO_2 is much larger than that of brine and rock. Typical rock compressibility values at depths of interest for CO_2 sequestration range from 10^{-11} to $5 \cdot 10^{-9}$ Pa^{-1} (Neuzil, 1986), but can be effectively larger if plastic deformation conditions are reached. Water compressibility is of the order of $4.5 \cdot 10^{-10}$ Pa^{-1}, which lies within the range of rock compressibility values. CO_2 compressibility ranges from 10^{-9} to 10^{-8} Pa^{-1} (Law and Bachu, 1996; Span and Wagner, 1996), one to two orders of magnitude greater than that of rock and water. Thus, CO_2 compressibility has a significant effect on the first term in the right-hand side of equation (3). However, the second term, which accounts for rock compressibility, can be neglected in the CO_2 rich zone, both because it is small and because the volume of rock occupied by CO_2 is orders of magnitude smaller than that affected by pressure buildup of the formation brine.

The situation is different in the region occupied by resident water. Water compressibility is at the low end of rock compressibilities at large depths. Moreover, its value is multiplied by porosity. Therefore, water compressibility will only play a relevant role

in high porosity stiff rocks, which are rare. In any case, the two compressibility terms can be combined in the brine saturated zone, yielding

$$\rho_w g \left(\phi c_w + c_r\right) \frac{\partial h_w}{\partial t} = S_s \frac{\partial h_w}{\partial t}, \tag{4}$$

where h_w is the hydraulic head of water, and S_s is the specific storage coefficient (Bear, 1972), which accounts for both brine and rock compressibility.

The specific storage coefficient controls, together with permeability, the radius of influence, R (i.e. the size of the pressure buildup cone caused by injection). In fact, assuming the aquifer to be large and for the purpose of calculating pressure buildup, this infinite compressible system can be replaced by an incompressible system whose radius grows as determined from the comparison between Thiem's solution (steady state) (Thiem, 1906) and Jacob's solution (transient) (Cooper and Jacob, 1946)

$$\Delta P_w = \frac{Q_0 \mu_w}{4\pi k d} \ln\left(\frac{R^2}{r^2}\right) = \frac{Q_0 \mu_w}{4\pi k d} \ln\left(\frac{2.25 k \rho_w g t}{\mu_w r^2 S_s}\right), \tag{5}$$

where Q_0 is the volumetric flow rate, μ_w is the viscosity of water, k is the intrinsic permeability of the aquifer, d is the aquifer thickness and r is radial distance. The radius of influence can then be defined from equation (5) as

$$R = \sqrt{\frac{2.25 k \rho_w g t}{\mu_w S_s}}. \tag{6}$$

CO_2 is lighter than brine and density differences affect flow via buoyancy. To quantify the relative influence of buoyancy we define a gravity number, N, as the ratio of gravity to viscous forces. The latter can be represented by the horizontal pressure gradient ($Q_0 \mu / (2\pi k r d)$), and the former by the buoyancy force ($\Delta \rho g$) in Darcy's law, expressed in terms of equivalent head. This would yield the traditional gravity number for incompressible flow (e.g. Lake (1989)). However, for compressible fluids, the boundary condition is usually expressed in terms of the mass flow rate, Q_m (Figure 2). Therefore, it is more appropriate to write Q_0 as Q_m / ρ. Hence, N becomes

$$N = \frac{k \Delta \rho g \bar{\rho_c} 2\pi r_c d}{\mu_c Q_m}, \tag{7}$$

where $\Delta \rho$ is the difference between the fluids density, $\bar{\rho_c}$ is a characteristic density, r_c is a characteristic length and Q_m is the CO_2 mass flow rate. Large gravity numbers ($N >> 1$) indicate that gravity forces dominate. Small gravity numbers ($N << 1$) indicate that viscous forces dominate. Gravity numbers close to one indicate that gravity and viscous forces are comparable.

The characteristic density can be chosen as the mean CO_2 density of the plume. The characteristic length depends on the scale of interest (Kopp et al, 2009). The gravity number increases with the characteristic length, thus increasing the relative importance of gravity forces with respect to viscous forces (Tchelepi and Orr Jr., 1994). This implies that, as the CO_2 plume becomes large, gravity forces will dominate far from the injection well.

These equations can be solved numerically, e.g. (Aziz and Settari, 2002; Chen et al, 2006; Pruess et al, 2004). However, creating a numerical model for each potential candidate site may require a significant cost. Alternatively, the problem can be solved analytically using some simplifications. The use of analytical solutions is useful because

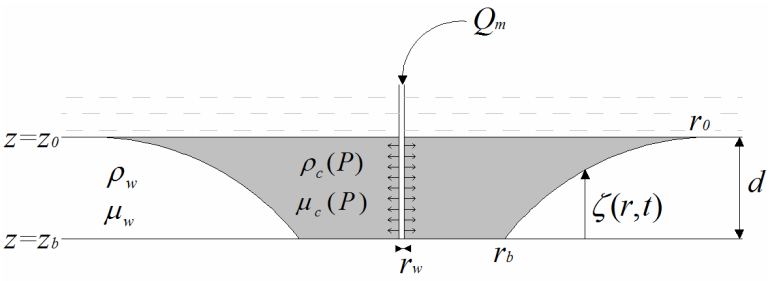

Fig. 2 Problem setup. Injection of compressible CO_2 in a homogeneous horizontal deep saline aquifer.

(i) they are instantaneous (Stauffer et al, 2009), (ii) numerical solutions can be coupled with analytical solutions to make them more efficient (Celia and Nordbotten, 2009) and (iii) they identify important scaling relationships that give insight into the balance of the physical driving mechanisms.

4 Analytical Solutions

4.1 Abrupt Interface Approximation

The abrupt interface approximation considers that the two fluids, CO_2 and brine in this case, are immiscible and separated by a sharp interface. The saturation of each fluid is assumed constant in each fluid region and capillary effects are usually neglected. Neglecting compressibility and considering a quasi-steady (successive steady-states) description of moving fronts in equation (2) yields that the volumetric flux defined in (1) is divergence free. Additionally, if the Dupuit assumption is adopted in a horizontal radial aquifer and S_α is set to 1, i.e. the α-phase relative permeability equals 1, the following equation can be derived (Bear, 1972)

$$\frac{1}{r}\frac{\partial}{\partial r}\left[\zeta\frac{Q_0 - 2\pi r\Delta\rho g(k/\mu_c)\,(d-\zeta)\,\partial\zeta/\partial r}{\zeta + (d-\zeta)\,\mu_w/\mu_c}\right] + 2\pi\phi\frac{\partial\zeta}{\partial t} = 0, \tag{8}$$

where ζ is the distance from the base of the aquifer to the interface position and Q_0 is the volumetric flow rate. To account for a residual saturation of the formation brine,

S_{r_w}, behind the CO_2 front, one should replace μ_c by $\mu_c/k_{r_c}^{'}$ in equation (8) and below, where $k_{r_c}^{'}$ is the CO_2 relative permeability evaluated at the residual brine saturation S_{r_w}. Equation (8) can be expressed in dimensionless form using

$$r_D = \frac{r}{r_c}, \quad \zeta_D = \frac{\zeta}{d}, \quad t_D = \frac{t}{t_c}, \quad M = \frac{k_{r_w}/\mu_w}{k_{r_c}/\mu_c}, \quad N, \tag{9}$$

where M is the mobility ratio, N is the gravity number defined in equation (7), t_c is the characteristic time and the subscript D denotes a dimensionless variable, which yields

$$\frac{1}{r_D}\frac{\partial}{\partial r_D}\left[\zeta_D \frac{1 - r_D N(d/r_c)\,(1-\zeta_D)\,\partial\zeta_D/\partial r_D}{\zeta_D + (1-\zeta_D)\,/M}\right] + \frac{\partial \zeta_D}{\partial t_D} = 0. \tag{10}$$

Equation (10) shows that the problem depends on two parameters, N and M. The mobility ratio will have values around 0.1 for CO_2 sequestration, which will lead to the formation of a thin layer of CO_2 along the top of the aquifer (Hesse et al, 2007, 2008; Juanes et al, 2009). On the other hand, the gravity number can vary over several orders of magnitude, depending on the aquifer permeability and the injection rate. Thus, the gravity number is the key parameter governing the interface position.

The analytical solutions of Nordbotten et al (2005) and Dentz and Tartakovsky (2009a) to determine the interface position of the CO_2 plume when injecting supercritical CO_2 in a deep saline aquifer start from this approximation.

4.2 Nordbotten et al (2005) Approach

To find the interface position, Nordbotten et al (2005) solve equation (8) neglecting the gravity term and approximating the transient system response to injection into an infinite aquifer by a solution to the steady-state problem with a moving outer boundary whose location increases in proportion to $\sqrt{t}$ in a radial geometry, i.e. the radius of influence defined in (6). In addition, they impose (i) volume balance, (ii) gravity override (CO_2 plume travels preferentially along the top) and (iii) they minimize energy at the well. The fluid pressure applies over the entire thickness of the aquifer and fluid properties are vertically averaged. The vertically averaged properties are defined as a linear weighting between the properties of the two phases. Nordbotten et al (2005) write their solution as a function of the mobility, λ_α, defined as the ratio of relative permeability to viscosity, $\lambda_\alpha = k_{r_\alpha}/\mu_\alpha$. For the case of an abrupt interface where both sides of the interface are fully saturated with the corresponding phase, the relative permeability is one and λ becomes the inverse of the viscosity of each phase. These viscosities are assumed constant.

Under these assumptions, Nordbotten et al (2005) obtain the interface position as,

$$\zeta_N(r,t) = d\left[1 - \frac{\mu_c}{\mu_w - \mu_c}\left(\sqrt{\frac{\mu_w V(t)}{\mu_c \phi \pi d r^2}} - 1\right)\right], \tag{11}$$

where $V(t) = Q_0 \cdot t$ is the CO_2 volume assuming a constant CO_2 density.

Integrating the flow equation and assuming vertically integrated properties of the fluid over the entire thickness of the formation, Nordbotten et al (2005) provide the following expression for fluid pressure buildup

$$\overline{P}_N(r,t) - \overline{P}_0 = \frac{Q_0 \mu_w}{2\pi k}\int_r^R \frac{\mathrm{d}r}{r\left[\left(\frac{\mu_w - \mu_c}{\mu_c}\right)(d - \zeta(r)) + d\right]}, \tag{12}$$

where $\overline{P}_N$ is the vertically averaged pressure, $\overline{P}_0$ is the vertically averaged initial pressure prior to injection, Q_0 is the volumetric CO_2 injection flow rate, k is the intrinsic permeability of the aquifer, r is the radial distance and R is the radius of influence.

4.3 Dentz and Tartakovsky (2009a) Approach

Dentz and Tartakovsky (2009a) also consider an abrupt interface approximation. They include buoyancy effects, and the densities and viscosities of each phase are assumed constant.

They combine Darcy's law with the Dupuit assumption in radial coordinates. Imposing fluid pressure continuity at the interface they obtain

$$\zeta_{DT}\left(r,t\right) = d\gamma_{cw} \ln\left[\frac{r}{r_b(t)}\right], \tag{13}$$

where r_b is the radius of the interface at the base of the aquifer and γ_{cw} is a dimensionless parameter that measures the relative importance of viscous and gravity forces

$$\gamma_{cw} = \frac{Q_0}{2\pi k d^2 g}\frac{\Delta\mu}{\Delta\rho}, \tag{14}$$

where $\Delta\mu = \mu_w - \mu_c$ is the difference between fluid viscosities and $\Delta\rho = \rho_w - \rho_c$ is the difference between fluid densities.

The interface radius at the base of the aquifer is obtained from volume balance as

$$r_b\left(t\right) = \sqrt{\frac{2Q_0 t}{\pi\phi d\gamma_{cw}}\left[exp\left(\frac{2}{\gamma_{cw}}\right) - 1\right]^{-1}}. \tag{15}$$

Note that the fluid viscosity contrast is treated differently in the two approaches (i.e. mobility ratio and viscosity difference). The mobility ratio is particularly relevant in multiphase flow when the two phases coexist. However, when one phase displaces the other, the viscosity difference governs the process (see equation (14) in Dentz and Tartakovsky (2009a) solution). An exception to this is the case when fluid properties are integrated vertically (Nordbotten et al, 2005), which can be thought of as a coexistence of phases.

5 Compressibility Correction

Let us assume that we have an initial estimation of the mean CO_2 density and viscosity. With this we can calculate the interface position using either analytical solutions (11) or (13). Furthermore, the fluid pressure can be calculated from Darcy's law. Then, the density can be determined within the plume assuming that it is solely a function of pressure. Integrating the CO_2 density within the plume and dividing it by the volume of the plume, we obtain the mean CO_2 density

$$\overline{\rho}_c = \frac{1}{V}\int_0^d \int_0^{r(\zeta)} 2\pi\phi r \rho_c(P_c)\mathrm{d}r\mathrm{d}z, \tag{16}$$

where V is the volume occupied by the CO_2 plume and $r(\zeta)$ is the distance from the well to the interface position from either Nordbotten et al (2005) or Dentz and Tartakovsky (2009a).

Note here that we do not specify *a priori* a particular relationship between density and pressure. We only specify that density is solely a function of pressure. CO_2 density also depends on temperature (Garcia, 2003). However, we neglect thermal effects within the aquifer, and take the mean temperature of the aquifer as representative of the system. This assumption is commonly used in CO_2 injection simulations (e.g. Law and Bachu (1996); Pruess and Garcia (2002)) and may be considered valid if CO_2 does not expand rapidly. If this happens, CO_2 will experience strong cooling due to the Joule-Thomson effect.

The relationship between pressure and density in equation (16) is in general non-linear. Moreover, pressure varies in space. Notice that the dependence is two-way: CO_2 density depends explicitly on fluid pressure, but fluid pressure also depends on density, because density controls the plume volume, and thus the fluid pressure through the volume of water that needs to be displaced. Therefore, an iterative scheme is needed to solve this non-linear problem. As density varies moderately with pressure, a Picard algorithm should converge, provided that the initial approximation is not too far from the solution.

The formulation of this iterative approach requires an expression for the spatial variability of fluid pressure for each of the two analytical solutions. In the approach of Nordbotten et al (2005), we obtain an expression for the vertically averaged pressure by introducing (11) into (12) and integrating. The expression for pressure depends on the region: close to the injection well, all fluid is CO_2; far away, all fluid is saline water; in between the two phases coexist with an abrupt interface between them,

$$
\begin{aligned}
&r > r_0; \quad \overline{P}_N(r,t) = \overline{P}_0 + \frac{Q_0\mu_w}{2\pi kd}\ln\left(\frac{R}{r}\right), \qquad (17)\\
&r_b \le r \le r_0; \quad \overline{P}_N(r,t) = \overline{P}_0 + \frac{Q_0\mu_w}{2\pi kd}\left[\ln\left(\frac{R}{r_0}\right) + \sqrt{\frac{\mu_c\phi\pi d}{\mu_w V(t)}}(r_0 - r)\right],\\
&r < r_b; \quad \overline{P}_N(r,t) = \overline{P}_0 + \frac{Q_0\mu_w}{2\pi kd}\left[\ln\left(\frac{R}{r_0}\right) + \sqrt{\frac{\mu_c\phi\pi d}{\mu_w V(t)}}(r_0 - r_b) + \frac{\mu_c}{\mu_w}\ln\left(\frac{r_b}{r}\right)\right],
\end{aligned}
$$

where r_0 is the radial distance where the interface intersects the top of the aquifer, r_b is the radial distance where the interface intersects the bottom of the aquifer, $\overline{P}_0 = P_{t_0} + \rho_w g d/2$ is the vertically averaged fluid pressure prior to injection, and P_{t_0} is the initial pressure at the top of the aquifer. Mathias et al (2008) come to a similar expression for fluid pressure, but they consider a slight compressibility in the fluids and rock instead of a radius of influence. The vertically averaged fluid pressure varies with the logarithm of the distance to the well in the regions where a single phase is present (CO_2 or brine). However, it varies linearly in the region where both phases coexist.

Fluid pressure can be obtained from the Dentz and Tartakovsky (2009a) approach by integrating (1), assuming hydrostatic pressure (Dupuit approximation) in the aquifer, and taking the interface position given by (13), which yields

$$r > r(\zeta_{DT}); \quad P_{DT}(r,z,t) = P_{t_0} + \rho_w g(d-z) + \frac{Q_0\mu_w}{2\pi kd}\ln\left(\frac{R}{r}\right), \tag{18}$$

$$r \le r(\zeta_{DT}); \quad P_{DT}(r,z,t) = P_{t_0} + \rho_w g(d-z) + \frac{Q_0}{2\pi kd}\left(\mu_w \ln\left(\frac{R}{r_b}\right) + \mu_c \ln\left(\frac{r_b}{r}\right) - (\mu_w - \mu_c)\frac{z}{d\gamma_{cw}}\right).$$

Equation (18) can be averaged over the entire thickness of the aquifer to obtain an averaged pressure, which will be used to compare the two approaches. This averaged pressure is given by

$$\begin{aligned}
&r > r_0; \quad \overline{P}_{DT}(r,t) = \overline{P}_0 + \frac{Q_0\mu_w}{2\pi kd}\ln\left(\frac{R}{r}\right),\\
&r_b \le r \le r_0; \quad \overline{P}_{DT}(r,t) = \overline{P}_0 + \frac{Q_0}{2\pi kd}\left[\mu_w\left[\ln\left(\frac{R}{r_b}\right) + \gamma_{cw}\ln\left(\frac{r}{r_b}\right)\ln\left(\frac{r_b}{r}\right)\right] + \right.\\
&\qquad \left. + \mu_c \ln\left(\frac{r_b}{r}\right)\left[1 - \gamma_{cw}\ln\left(\frac{r}{r_b}\right)\right] - \frac{\mu_w - \mu_c}{2\gamma_{cw}}\left[1 - \gamma_{cw}^2\left(\ln\left(\frac{r}{r_b}\right)\right)^2\right]\right],\\
&r < r_b; \quad \overline{P}_{DT}(r,t) = \overline{P}_0 + \frac{Q_0}{2\pi kd}\left[\mu_w \ln\left(\frac{R}{r_b}\right) + \mu_c \ln\left(\frac{r_b}{r}\right) - \frac{\mu_w - \mu_c}{2\gamma_{cw}}\right].
\end{aligned} \tag{19}$$

Thus, the vertically averaged fluid pressure is defined in three regions in both approaches by equations (17) and (19). Unsurprisingly, the two approaches have the same solution in the regions where only one phase exists. Differences appear in the region where CO_2 and the formation brine coexist. In the Nordbotten et al (2005) approach, the vertically averaged pressure varies linearly with distance to the well. However, in Dentz and Tartakovsky (2009a), it changes logarithmically with distance to the well. As a result, the approach of Dentz and Tartakovsky (2009a) predicts higher fluid pressure values in this zone.

Equations (17) and (18) allow us to develope a simple iterative method for correcting the interface position. The method can be applied to both the Nordbotten et al (2005) and Dentz and Tartakovsky (2009a) solutions as well as to any other future solutions that may emerge. The procedure is as follows

1. Take a reasonable initial approximation for mean CO_2 density and viscosity from the literature, e.g. Bachu (2003).
2. Determine the interface position using mean density and viscosity in analytical solutions (11) or (13).
3. Calculate the pressure distribution using (17) or (18).
4. Calculate the corresponding mean density and viscosity of the CO_2 using (16).
5. Repeat steps 2-4 until the solution converges to within some prespecified tolerance. Two different convergence criteria can be chosen: (i) changes in the interface position or (ii) changes in the mean CO_2 density.

The method is relatively easy to implement and can be programmed in a spreadsheet or any code of choice. The method converges rapidly, within a few iterations (typically less than 5) in all test cases. A calculation spreadsheet can be downloaded from GHS (2009).

6 Application

6.1 Injection scenarios

To illustrate the relevance of CO_2 compressibility effects, we consider three injection scenarios: (i) a regime in which viscous forces dominate gravity forces, (ii) one where both forces have a similar influence and (iii) a case where gravity forces dominate.

CO_2 thermodynamic properties have been widely investigated, e.g. (Sovova and Prochazka, 1993; Span and Wagner, 1996; Garcia, 2003). The thermodynamic properties given by Span and Wagner (1996) are almost identical to the International Union of Pure and Applied Chemistry (IUPAC) (Angus et al, 1976) data sets over the $P-T$ range of CO_2 sequestration interest (McPherson et al, 2008). However, the algorithm given by Span and Wagner (1996) for evaluating CO_2 properties has a very high computational cost. For the sake of simplicity and illustrative purposes, we assume a linear relationship between CO_2 density and pressure, given as

$$\rho_c = \rho_0 + \rho_1 \beta (P_c - P_{t_0}), \tag{20}$$

where ρ_0 and ρ_1 are constants for the CO_2 density, β is the CO_2 compressibility, P_c is CO_2 pressure and P_{t_0} is the reference pressure for ρ_0. ρ_0, ρ_1 and β are obtained from data tables in Span and Wagner (1996). Appendix A contains the expressions for the mean CO_2 density using this linear approximation in (20) for both approaches.

CO_2 viscosity is calculated using an expression proposed by Altunin and Sakhabetdinov in 1972 (Sovova and Prochazka, 1993). In this expression, the viscosity is a function of density and temperature. Thus the mean CO_2 viscosity is calculated from the mean CO_2 density. Figure 3 shows how the density varies within the CO_2 plume for one of our numerical simulations. The numerical simulations calculate CO_2 density by means of an exponential function (Span and Wagner, 1996) and CO_2 viscosity using the same expression as here (Altunin and Sakhabetdinov (1972), in Sovova and Prochazka (1993)). The maximum error encountered in this study due to the linear CO_2 density approximation was around 8 %, which we deem acceptable for our illustrative purposes. Bachu (2003) shows vertical profiles of CO_2 density assuming hydrostatic pressure and different geothermal gradients. However, pressure buildup affects CO_2 properties. Hence, these vertical profiles can only be taken as a reference, for example, to obtain the initial approximation of CO_2 density and viscosity.

We study a saline aquifer at a depth that ranges from 1000 to 1100 m. The temperature is assumed to be constant and equal to 320 K. For this depth and temperature, the initial CO_2 density is estimated as 730 kg/m^3 (Bachu, 2003). The corresponding CO_2 viscosity according to Altunin and Sakhabetdinov is 0.061 mPa·s.

For the numerical simulations we used the program CODE_BRIGHT (Olivella et al, 1994, 1996) with the incorporation of the above defined constitutive equations for CO_2 density and viscosity. This code solves the mass balance of water and CO_2 (equation (2)) using the Finite Element Method and a Newton-Raphson scheme to solve the non-linearities. The aquifer is represented by an axysimetric model in which a constant CO_2 mass rate is injected uniformly in the whole vertical of the well. The aquifer is assumed infinite-acting, homogeneous and isotropic. In order to obtain a solution close to an abrupt interface, a van Genuchten retention curve (van Genuchten, 1980), with an entry pressure, P_o, of 0.02 MPa and the shape parameter $\lambda = 0.8$, was used. To approximate a sharp interface, linear relative permeability functions, for both the CO_2

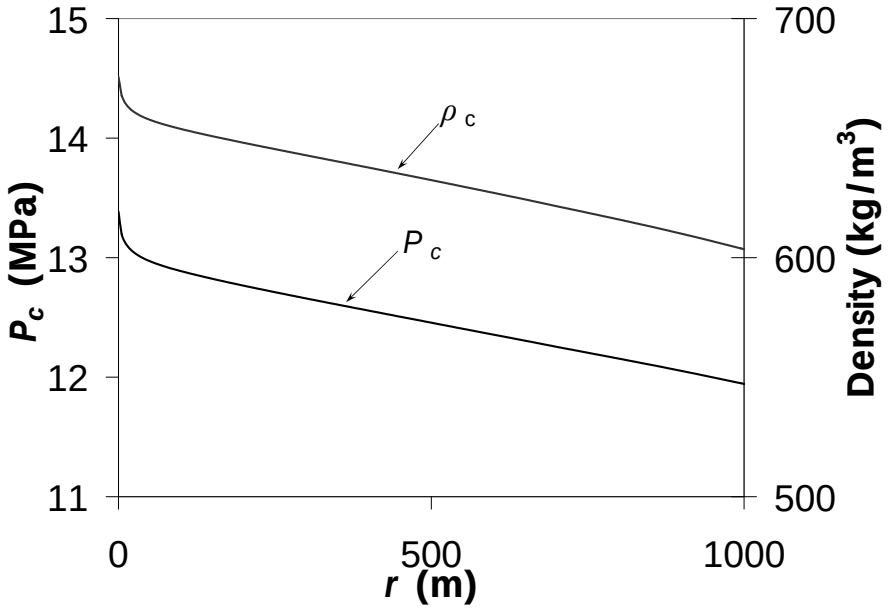

Fig. 3 CO_2 pressure and CO_2 density at the top of the aquifer resulting from a numerical simulation that acknowledges CO_2 compressibility.

and the brine, have been used (Table 1). This retention curve and relative permeability functions enable us to obtain a CO_2 rich zone with a saturation very close to 1, and a relatively narrow mixing zone. The CO_2 saturation 90 % iso-line has been chosen to represent the position of the interface.

Table 1. Parameters considered for the numerical simulations in the three injection scenarios.

	λ	P_o	k	k_{r_α}	Q_m	r_w	S
	-	MPa	m^2	-	kg/s	m	-
Case 1			10^{-13}		120		
Case 2	0.8	0.02	10^{-12}	S_α	79	0.15	0.0001
Case 3			10^{-12}		1		

6.2 Case 1: Viscous Forces Dominate

This first case consists of an injection with a gravity number of the order of 10^{-3} in the well. In this situation, the corrected mean CO_2 density (770 kg/m^3 for Nordbotten et al (2005) and 803 kg/m^3 for Dentz and Tartakovsky (2009a)) is higher than that assumed initially (730 kg/m^3). The corresponding CO_2 viscosities are 0.067 and 0.073 mPa·s respectively. Therefore, the corrected interface position is located closer to the well than when we neglect variations in density. The Dentz and Tartakovsky (2009a)

approach gives a higher value of the mean CO_2 density because fluid pressure grows exponentially, while it grows linearly in Nordbotten et al (2005) approach, thus leading to lower fluid pressure values in the zone where CO_2 and brine coexist. We define relative error, E_{rel}, of the interface position as

$$E_{rel} = \frac{R_i - R_c}{R_i}, \tag{21}$$

where R_i is the radius of the CO_2 plume at the top of the aquifer for incompressible CO_2 and R_c is the radius of the CO_2 plume at the top of the aquifer for compressible CO_2.

Differences between the compressible and incompressible solutions are shown in Figure 4. For the Dentz and Tartakovsky (2009a) solution, the relative error increases slightly from the base to the top of the aquifer, presenting a maximum relative error of 6 % at the top of the aquifer. For the Nordbotten et al (2005) solution the interface tilts, with the base of the interface located just 2 % further from the well than its initial position, but the top positioned 7 % closer to the well. The difference in shape between the two analytical solutions results in a CO_2 plume that extends further along the top of the aquifer for Nordbotten et al (2005) solution than Dentz and Tartakovsky (2009a) over time (Figure 4b). A similar behavior can be seen in the numerical simulations (Figure 4a). In this case, the interface given by the numerical simulation compares favourably with that of Nordbotten et al (2005).

Figure 4c displays a comparison between the vertically averaged fluid pressure given by both approaches. The fluid pressure given by Mathias et al (2008) is almost identical to that obtained in Nordbotten et al (2005) approach (equation (17)). This is because Mathias et al (2008) assumed the Nordbotten et al (2005) solution for the interface position and that the hypothesis made therein are valid. The minor difference in fluid pressure between these two expressions comes from considering a slight fluid and rock compressibility beyond the plume (recall Section 3). Thus, both expressions can be considered equivalent for the vertically averaged fluid pressure. Fluid pressure obtained from the numerical simulation is smaller than the other profiles inside the CO_2 plume region. This may reflect the larger energy dissipation produced by analytical solutions as a result of the Dupuit assumption.

6.3 Case 2: Comparable Gravity and Viscous Forces

Here, the gravity number at the well is in the order of 10^{-1} (Note that the gravity number increases to 1 if we take a characteristic length only 1.5 m away from the injection well. In fact, it keeps increasing further away from the well, where gravity forces will eventually dominate (recall Section 3)). The density variations between the initial guess of 730 kg/m^3 and the corrected value can be large. The density reduces to 512 kg/m^3 (viscosity of 0.037 mPa·s) for Nordbotten et al (2005) and to 493 kg/m^3 (viscosity of 0.036 mPa·s) for Dentz and Tartakovsky (2009a). This means that the error associated with neglecting CO_2 compressibility can become very large and should be reflected in the interface position (Figure 5a). For the Dentz and Tartakovsky (2009a) solution including compressibility leads to a 26 % error at the top of the aquifer. This relative error reaches 53 % in the Nordbotten et al (2005) solution. Over a 30 year injection this could represent a potential error of 3 km in the interface position estimation (Figure 5b). Here, the numerical simulations also show the importance of

considering CO_2 compressibility. The interface position from the simulations is similar to that of Nordbotten et al (2005) in the lower half of the aquifer, where viscous forces may dominate, but it is similar to that of Dentz and Tartakovsky (2009a) in the upper part of the aquifer, where buoyancy begins to dominate.

This dominant buoyancy flow may be significant when considering risks associated with potential leakage from the aquifer (Nordbotten et al, 2009) or mechanical damage of the caprock (Vilarrasa et al, 2010), where the extent and pressure distribution of the CO_2 on the top of the aquifer plays a dominant role.

Unlike the previous case, the mean CO_2 density of Dentz and Tartakovsky (2009a) approach is lower than that of Nordbotten et al (2005). This is because Nordbotten et al (2005) consider the vertically averaged fluid pressure (Figure 5c). When gravity forces play an important role, the CO_2 plume largely extends at the top of the aquifer. CO_2 pressure at the top of the aquifer is lower than the vertically averaged fluid pressure, which considers CO_2 and the formation brine. Thus, the mean CO_2 density is overestimated when it is calculated from vertically averaged fluid pressure values.

6.4 Case 3: Gravity Forces Dominate

In this case, the gravity number is close to 10 at the well. Density deviations from our initial guess can be very large here. The mean density drops to 479 kg/m^3 for Nordbotten et al (2005) and to 449 kg/m^3 for Dentz and Tartakovsky (2009a) solutions, which correspond to CO_2 viscosities of 0.035 and 0.032 mPa·s respectively. This means that the interface position at the top of the aquifer will extend much further than when not considering CO_2 compressibility. The Dentz and Tartakovsky (2009a) solution clearly reflects buoyancy and the CO_2 advances through a very thin layer at the top of the aquifer (Figure 6a). In contrast, the Nordbotten et al (2005) interface cannot represent this strong buoyancy effect because this solution does not account for gravitational forces. The relative error of the interface position at the top of the aquifer is of 30 % for Dentz and Tartakovsky (2009a) solution, and of 64 % for Nordbotten et al (2005). In this case, the numerical simulation compares more favourably with the Dentz and Tartakovsky (2009a) solution.

The vertically averaged pressure from Dentz and Tartakovsky (2009a) is similar to that of the numerical simulation because gravity forces dominate (Figure 6c). In this case, Nordbotten et al (2005) predict a very small pressure buildup, which reflects their linear variation with distance. In addition, the zone with only CO_2, where fluid pressure grows logarithmically, is very limited.

Finally, we consider the influence of the gravity number on CO_2 compressibility effects. Figure 7 displays the relative error (Equation (21)) of the interface position at the top of the aquifer as a function of the gravity number, computed at the injection well. Negative relative errors mean that the interface position extends further when considering CO_2 compressibility. Both analytical solutions, i.e. Nordbotten et al (2005) and Dentz and Tartakovsky (2009a), present a similar behaviour, but Nordbotten et al (2005) has a bigger error. This is mainly because they vertically average fluid pressure, which leads to unrealistic CO_2 properties in the zone where both CO_2 and brine exist. For gravity numbers greater than 1, the mean CO_2 density tends to a constant value because fluid pressure buildup in the well is very small. For this reason, the relative error remains constant for this range of gravity numbers. However, the absolute relative error decreases until the mean CO_2 density equals that of the initial approximation for

gravity numbers lower than 1. The closer the initial CO_2 density approximation is to the actual density, the smaller is the error in the interface position.

Figure 8 displays the mean CO_2 density as a function of the gravity number computed in the well for the cases discussed here. Differences arise between the two analytical approaches. The most relevant difference occurs at high gravity numbers. For gravity numbers greater than $5 \cdot 10^{-2}$, Nordbotten et al (2005) yield a higher CO_2 density because fluid pressure is averaged over the whole vertical. Thus, fluid pressure in the zone where CO_2 and brine exist is overestimated, resulting in higher CO_2 density values. For gravity numbers lower than $5 \cdot 10^{-2}$, CO_2 density given by Dentz and Tartakovsky (2009a) is slightly higher than that of Nordbotten et al (2005) because the former predicts higher fluid pressure values in the CO_2 rich zone, as explained previously. However, both approaches present similar mean CO_2 density values for low gravity numbers.

7 Summary and Conclusions

CO_2 compressibility effects may play an important role in determining the size and geometry of the CO_2 plume that will develop when supercritical CO_2 is injected in an aquifer. Here, we have studied the effect that accounting for CO_2 compressibility (density variations and corresponding changes in viscosity) exerts on he shape of the plume computed by two abrupt interface analytical solutions. To this end, we have presented a simple method to correct the initial estimation of the CO_2 density and viscosity and hence use more realistic values. These corrected values give a more accurate prediction for the interface position of the CO_2 plume.

The error associated with neglecting compressibility increases dramatically when gravity forces dominate, which is likely to occur at late injection times. This is relevant because the relative importance of buoyancy forces increases with distance to the injection well. Thus gravity forces will ultimately dominate in most CO_2 sequestration projects. As such incorporating CO_2 compressibility is critical for determining the interface position.

Comparison with numerical simulations suggests that the solution by Nordbotten et al (2005) gives good predictions when viscous forces dominate, while the Dentz and Tartakovsky (2009a) solution provides good estimates of the CO_2 plume position when gravity forces dominate.

8 Appendix A

Here, the mean CO_2 density defined in (16) is calculated using the linear approximation of CO_2 density with respect to pressure presented in (20) for both approaches, i.e. Nordbotten et al (2005) and Dentz and Tartakovsky (2009a).

With the Nordbotten et al (2005) approach, the mean CO_2 density is calculated by introducing (11) and (17) into (16), which leads to

$$\overline{\rho}_{c_N} = \frac{2\pi\phi}{V}\left\{\rho_0\frac{d}{2}r_0r_b+\rho_1\beta\left[\frac{r_0r_b}{4}\rho_w g d^2+\frac{Q_0\mu_w}{2\pi k}\left[r_0r_b\left(\frac{1}{2}\ln\left(\frac{R}{r_0}\right)+\frac{1}{3}\right)-\frac{r_b^2}{6}\left(1-\frac{1}{2}\frac{\mu_c}{\mu_w}\right)\right]\right]\right\}. \tag{22}$$

Similarly, introducing (13) and (18) into (16), and integrating, yields the expression for the mean CO_2 density for the Dentz and Tartakovsky (2009a) approach,

$$\overline{\rho}_{c_{DT}} = \frac{2\pi\phi}{V}\left\{ \left(e^{(2/\gamma_{cw})}-1\right)\frac{r_b^2}{4}d\gamma_{cw}\left[\rho_0+\rho_1\beta\left(\frac{d\gamma_{cw}}{2}\rho_w g+\frac{Q_0}{2\pi kd}\left(\mu_w \ln\left(\frac{R}{r_b}\right)+\frac{\mu_w+\mu_c}{2}\right)\right)\right] \right.$$
$$\left. -\frac{r_b^2}{4}d^2\gamma_{cw}\rho_1\beta\rho_w g - e^{(2/\gamma_{cw})}\frac{r_b^2}{4}d\rho_1\beta\frac{Q_0}{2\pi kd}\mu_w \right\}. \quad (23)$$

Acknowledgements V.V. and D.B want to acknowledge the Spanish Ministry of Science and Innovation (MCI) for financial support through the "Formación de Profesorado Universitario" and "Juan de la Cierva" programs. V.V. also wants to acknowledge the "Colegio de Ingenieros de Caminos, Canales y Puertos - Catalunya" for their financial support. Additionally, we would like to acknowledge the 'CIUDEN' project (Ref.: 030102080014), the 'PSE' project (Ref.: PSE-120000-2008-6), the 'COLINER' project and the 'MUSTANG' project (from the European Community's Seventh Framework Programme FP7/2007-2013 under grant agreement n^o 227286) for their financial support.

References

Angus A, Armstrong B, Reuck KM (ed) (1976) International thermodynamics tables of the fluid state. Carbon dioxide. International Union of Pure and Applied Chemistry. Pergamon Press, Oxford

Aziz K, Settari A (ed) (2002) Petroleum Reservoir Simulation. Blitzprint Ltd., 2nd edition

Bachu S (2003) Screening and ranking of sedimentary basins for sequestration of CO_2 in geological media in response to climate change. Environmental Geology 44:277–289

Bachu S, Adams JJ (2003) Sequestration of CO_2 in geological media in response to climate change: capacity of deep saline aquifers to sequester CO_2 in solution. Energy Conversion & Management 44:3151–3175

Bear J (ed) (1972) Dynamics of Fluids in Porous Media. Elsevier, New York

Bolster D, Barahona M, Dentz M, Fernandez-Garcia D, Sanchez-Vila X, Trinchero P, Valhondo C, Tartakovsky DM (2009a) Probabilistic risk analysis of groundwater remediation strategies. Water Resour Res, in press

Bolster D, Dentz M, Carrera J (2009b) Effective two phase flow in heterogeneous media under temporal pressure fluctuations. Water Resour Res 45:W05,408, doi:10.1029/2008WR007,460

Cantucci B, Montegrossi G, Vaselli O, Tassi F, Quattrocchi F, Perkins EH (2009) Geochemical modeling of CO_2 storage in deep reservoirs: The Weyburn Project (Canada) case study. Chemical Geology 265:181–197

Celia MA, Nordbotten JM (2009) Practical modeling approaches for geological storage of carbon dioxide. Ground Water 47 (5):627–638

Cooper HH, Jacob CE (1946) A generalized graphical method for evaluating formation constants and summarizing well field history. American Geophysical Union Trans. 27:526–534.

Chen Z, Huan G, Ma Y (ed) (2006) Computational methods for multiphase flows in porous media. SIAM, Philadelphia

Dake LP (ed) (1978) Fundamentals of Reservoir Engineering. Elsevier, Oxford

Dentz M, Tartakovsky DM (2009a) Abrupt-interface solution for carbon dioxide injection into porous media. Transport In Porous Media 79:15-27

Dentz M, Tartakovsky DM (2009b) Response to "Comments on abrupt-interface solution for carbon dioxide injection into porous media by Dentz and Tartakovsky (2008)" by Lu et al. Transport In Porous Media 79:39-41

Ennis-King J, Paterson L (2005) The role of convective mixing in the long-term storage of carbon dioxide in deep saline formations. Journal of Society of Petroleum Engineers 10(3):349–356

Garcia JE (2003) Fluid Dynamics of Carbon Dioxide Disposal into Saline Aquifers. PhD thesis, University of California, Berkeley

Garcia JE, K Pruess (2003) Flow Instabilities during injection of CO_2 into saline aquifers. Proceedings Tough Symposium 2003, LBNL, Berkeley

GHS (2009) Spreadsheet with CO_2 compressibility correction. http://www.h2ogeo.upc.es/publicaciones/2009/Transport%20in%20porous%20media/Effects%20of%20CO2%20Compressibility%20on%20CO2%20Storage%20in%20Deep%20Saline%20Aquifers.xls.

Hesse MA, Tchelepi HA, Cantwell BJ, Orr Jr. FM (2007) Gravity currents in horizontal porous layers: Transition from early to late self-similarity. Journal of Fluid Mechanics 577:363–383

Hesse MA, Tchelepi HA, Orr Jr. FM (2008) Gravity currents with residual trapping. Journal of Fluid Mechanics 611:35–60

Hidalgo JJ, Carrera J (2009) Effect of dispersion on the onset of convection during CO_2 sequestration. Journal of Fluid Mechanics 640:443–454

Hitchon B, Gunter WD, Gentzis T, Bailey RT (1999) Sedimentary basins and greenhouse gases: a serendipitous association. Energy Conversion & Management 40:825–843

Huppert HE, Woods AW (1995) Gravity-driven flows in porous media. Journal of Fluid Mechanics 292:55–69

Juanes R, MacMinn CW, Szulczewski ML (2009) The footprint of the CO_2 plume during carbon dioxide storage in saline aquifers: Storage efficiency for capillary trapping at the basin scale. Transport In Porous Media DOI 10.1007/s11242-009-9420-3

Katz DL, Lee RL (ed) (1990) Natural gas engineering. McGraw-Hill, New York

Korbol R, Kaddour A (1995) Sleipner vest CO_2 disposal - injection of removed CO_2 into the Utsira formation. Energy Conversion Management 36 (6-9):509–512

Kopp A, Class H, Helmig R (2009) Investigation on CO_2 storage capacity in saline aquifers Part 1. Dimensional analysis of flow processes and reservoir characteristics. Journal of Greenhouse Gas Control 3:263–276

Lake LW (ed) (1989) Enhanced Oil Recovery. Prentice-Hall, Englewood Cliffs, New Jersey

Law DHS, Bachu S (1996) Hydrogeological and numerical analysis of CO_2 disposal in deep aquifers in the Alberta sedimentary basin. Energy Conversion & Management 37(6-8):1167–1174

Lu C, Lee S-Y, Han WS, McPherson BJ, Lichtner PC (2009) Comments on "abrupt-interface solution for carbon dioxide injection into porous media" by M. Dentz and D. Tartakovsky. Transport In Porous Media 79:29-37

Lyle S, Huppert HE, Hallworth M, Bickle M, Chadwick A (2005) Axisymmetric gravity currents in a porous medium. Journal of Fluid Mechanics 543:293–302

Mathias SA, Hardisty PE, Trudell MR, Zimmerman RW (2008) Approximate solutions for pressure buildup during CO_2 injection in brine aquifers. Transport In Porous Media doi 10.1007/s11242-008-9316-7

McPherson BJOL, Han WS, Cole BS (2008) Two equations of state assembled for basic analysis of multiphase CO_2 flow and in deep sedimentary basin conditions. Computers and Geosciences 34:427–444

Neuweiller I, Attinger S, Kinzelbach W, King P (2003) Large scale mixing for immiscible displacement in heterogenous porous media. Transport In Porous Media 51:287–314

Neuzil CE (1986) Groundwater flow in low-permeability environments. Water Resources Research 22(8):1163–1195

Nooner SL, Eiken O, Hermanrud C, Sasagawa GS, Stenvold T, Zumberge MA (2007) Constraints on the *in situ* density of CO_2 within the Utsira formation from time-lapse seafloor gravity measurements. Journal of Greenhouse Gas Control 1:198–214

Nordbotten JM, Celia MA, Bachu S (2005) Injection and storage of CO_2 in deep saline aquifers: analytical solution for CO_2 plume evolution during injection. Transport In Porous Media 58:339–360

Nordbotten JM, Kavetski D, Celia MA, Bachu S (2009) A semi-analytical model estimating leakage associated with CO_2 storage in large-scale multi-layered geological systems with multiple leaky wells. Environmental Science & Technology 43(3):743–749 doi:10.1021/es801,135v

Olivella S, Carrera J, Gens A, Alonso EE (1994) Non-isothermal multiphase flow of brine and gas through saline media. Transport In Porous Media 15:271–293

Olivella S, Gens A, Carrera J, Alonso EE (1996) Numerical formulation for a simulator (CODE_BRIGHT) for the coupled analysis of saline media. Engineering Computations 13:87–112

Pruess K, Garcia J (2002) Multiphase flow dynamics during CO_2 disposal into saline aquifers. Environmental Geology 42:282–295

Pruess K, Garcia J, Kovscek T, Oldenburg C, Rutqvist J, Steelfel C, Xu T (2004) Code intercomparison builds confidence in numerical simulation models for geologic disposal of CO_2. Energy 29:1431–1444

Riaz A, Hesse M, Tchelepi H, Orr Jr FM (2006) Onset of convection in a gravitationally unstable diffusive boundary layer in porous media. Journal of Fluid Mechanics 548:87–111

Rutqvist J, Birkholzer J, Cappa F, Tsang C-F (2007) Estimating maximum sustainable geological sequestration of CO_2 using coupled fluid flow and geomechanical fault-slip analysis. Energy Conversion and Management 48:1798–1807

Saripalli P, McGrail P (2002) Semi-analytical approaches to modeling deep well injection of CO_2 for geological sequestration. Energy Conversion & Management 43:185–198

Sovova H, Prochazka J (1993) Calculations of compressed carbon dioxide viscosities. Ind Eng Chem Res 32 (12):3162–3169

Span R, Wagner W (1996) A new equation of state for carbon dioxide covering the fluid region from the triple-point to 1100 K at pressures up to 88 MPa. Journal Phys Chem Ref Data 25 (6):1509–1596

Stauffer PH, Viswanathan HS, Pawar RJ, Guthrie GD (2009) A system model for geologic sequestration of carbon dioxide. Environmental Science and Technology 43 (3):565–570

Thiem G (ed) (1906) Hydrologische Methode.Leipzig, Gebhardt

Tsang C-F, Birkholzer J, Rutqvist J (2008) A comparative review of hydrologic issues involved in geologic storage of CO_2 and injection disposal of liquid waste. Environmental Geology 54:1723–1737

Tartakovsky DM (2007) Probabilistic risk analysis in subsurface hydrology. Geophys Res Lett 34:L05,404

Tchelepi HA, Orr Jr. FM (1994) Interaction of viscous fingering, permeability inhomogeneity and gravity segregation in three dimensions. SPE Symposium on Reservoir Simulation, New Orleans:266–271

van Genuchten MT (1980) A closed-form equation for predicting the hydraulic conductivity of unsaturated soils. Soil Sci Soc Am J 44:892–898

Vilarrasa V, Bolster D, Olivella S, Carrera J (2010) Coupled hydromechanical modelling of CO_2 sequestration in deep saline aquifers. International Journal of Greenhouse Gas Control, Submitted

Zhou Q, Birkholzer J, Tsang C-F, Rutqvist J (2008) A method for quick assessment of CO_2 storage capacity in closed and semi-closed saline formations. Journal of Greenhouse Gas Control Submitted 2:626–639

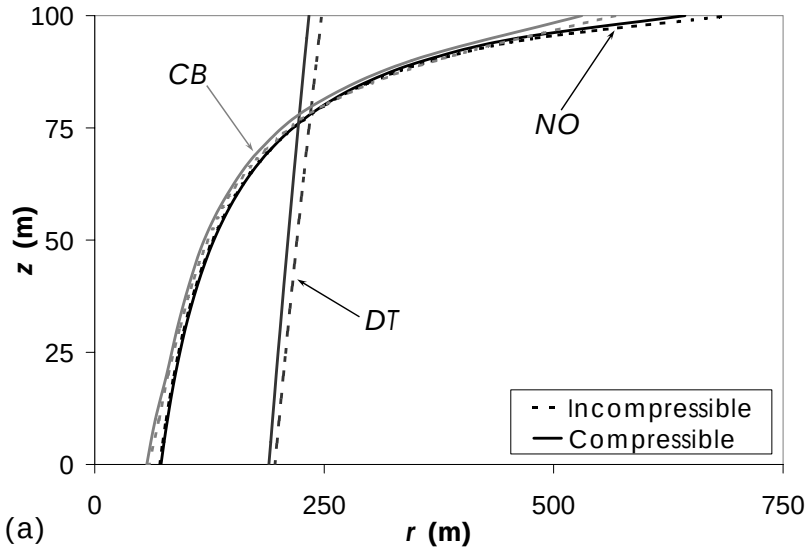

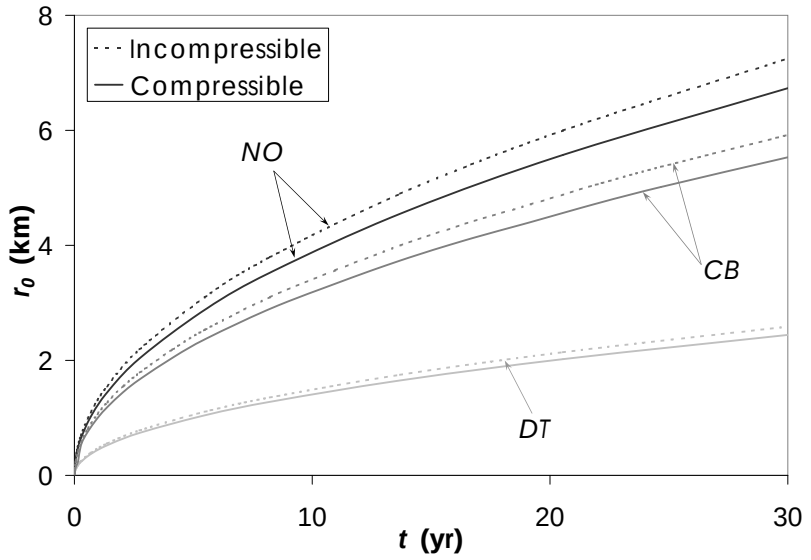

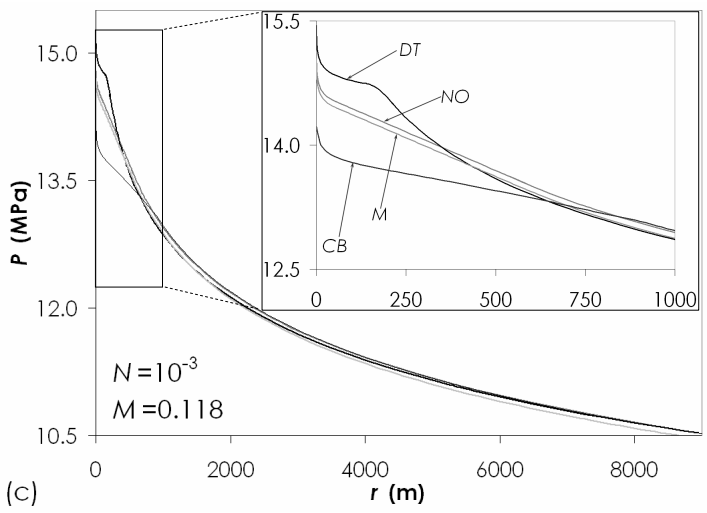

Fig. 4 Case 1: Viscous forces dominate. Gravity number, N, equals 10^{-3} in the well. (a) Abrupt interface position in a vertical cross section after 100 days of injection, (b) evolution of the CO_2 plume radius at the top of the aquifer and (c) vertically averaged fluid pressure with distance to the well after 100 days of injection, with a detail of the CO_2 rich zone. *NO* refers to Nordbotten et al (2005) solution, *DT* to Dentz and Tartakovsky (2009a) solution, *CB* to the numerical solution of CODE_BRIGHT and *M* is the Mathias et al (2008) solution for fluid pressure.

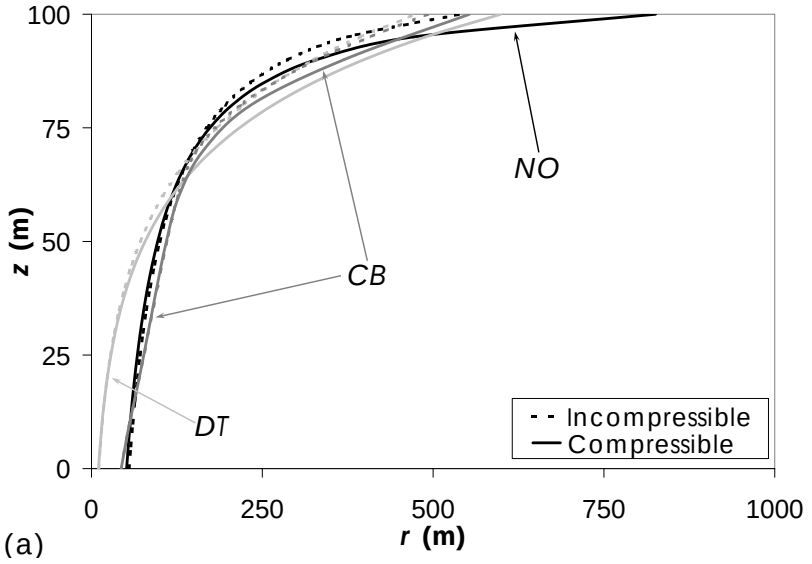

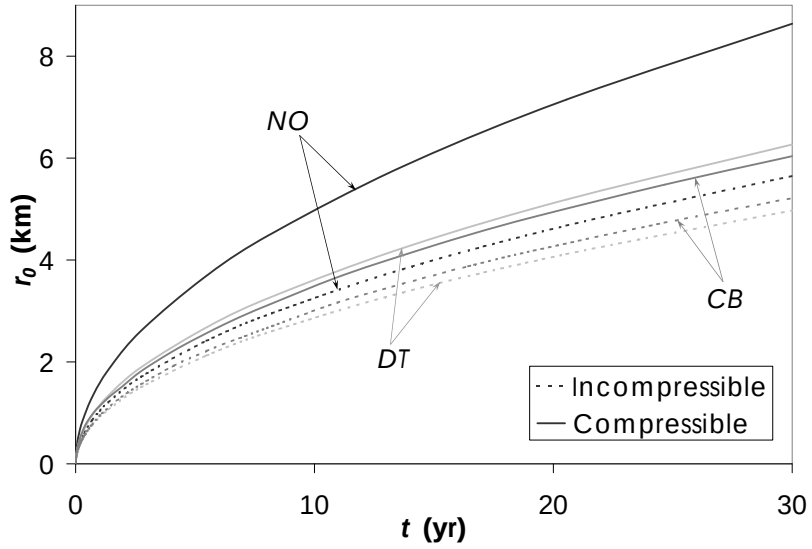

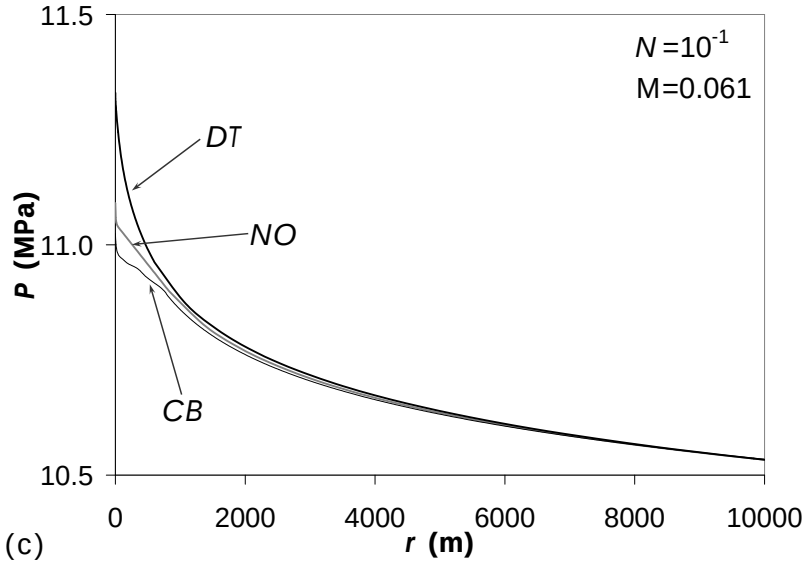

Fig. 5 Case 2: Comparable viscous and gravity forces. Gravity number, N, equals 10^{-1} in the well. (a) Abrupt interface position in a vertical cross section after 100 days of injection, (b) evolution of the CO_2 plume radius at the top of the aquifer and (c) vertically averaged fluid pressure with distance to the well after 100 days of injection. *NO* refers to Nordbotten et al (2005) solution, *DT* to Dentz and Tartakovsky (2009a) solution and *CB* to the numerical solution of CODE_BRIGHT.

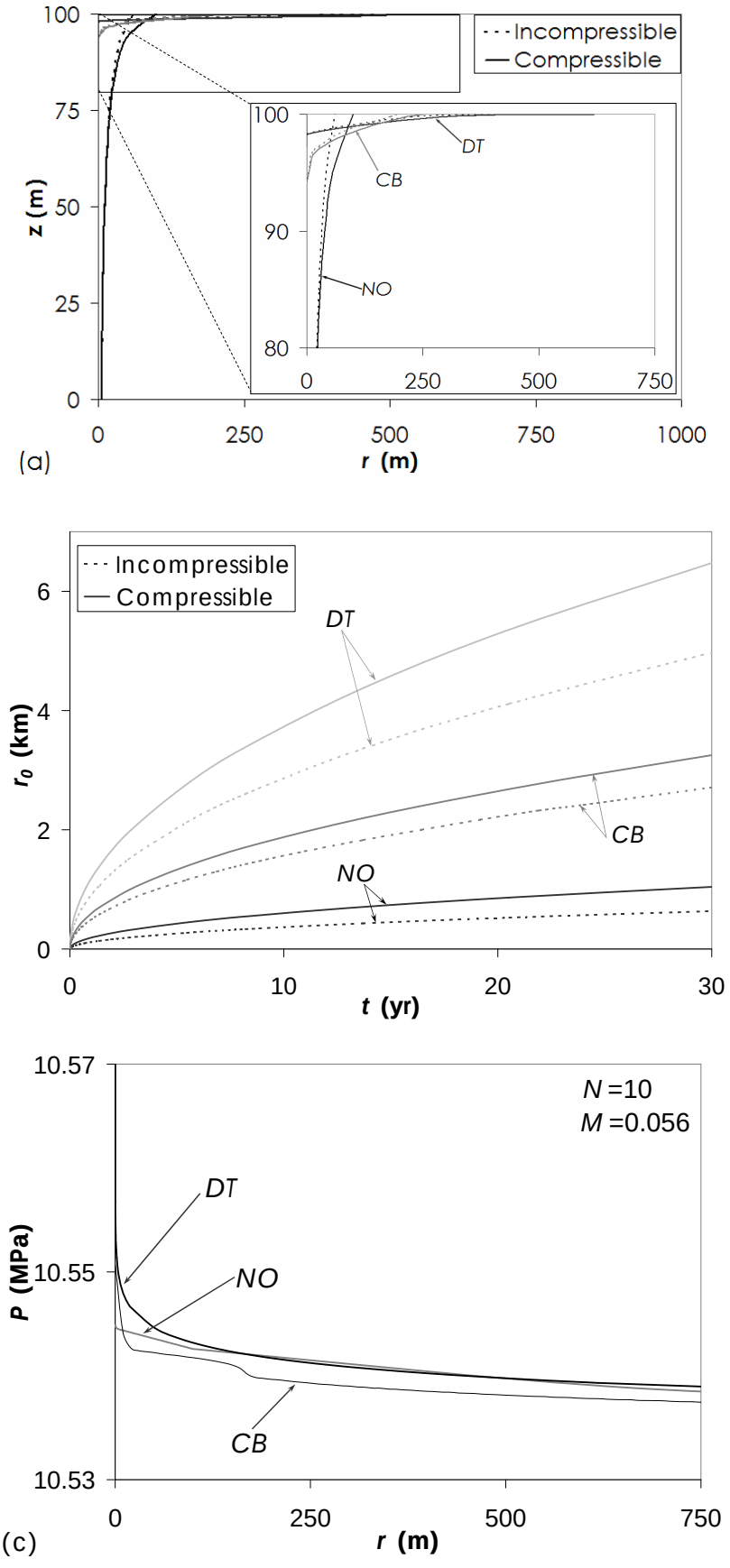

Fig. 6 Case 3: Gravity forces dominate. Gravity number, N, equals 10 in the well. (a) Abrupt interface position in a vertical cross section after 100 days of injection, (b) evolution of the CO_2 plume radius at the top of the aquifer and (c) vertically averaged fluid pressure with distance to the well after 100 days of injection. *NO* refers to Nordbotten et al (2005) solution, *DT* to Dentz and Tartakovsky (2009a) solution and *CB* to the numerical solution of CODE_BRIGHT.

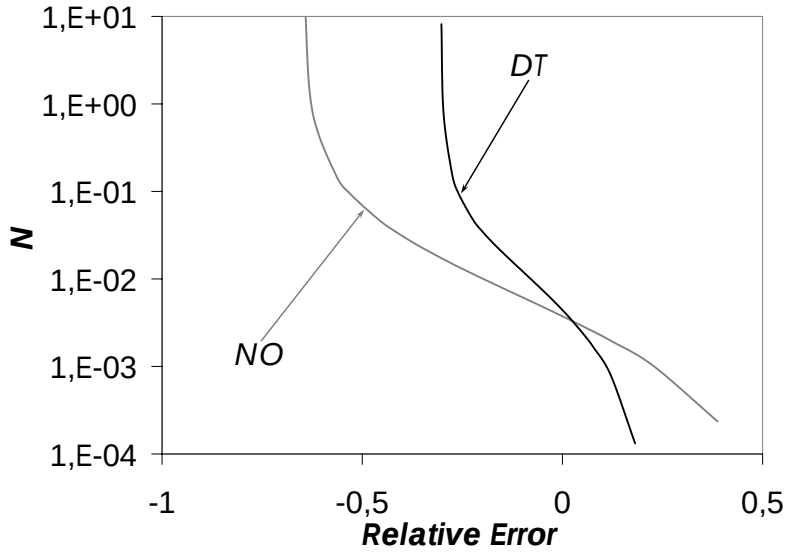

Fig. 7 Relative error (Equation (21)) of the interface position at the top of the aquifer made when CO_2 compressibility is not considered as a function of the gravity number for both analytical solutions. *NO* refers to Nordbotten et al (2005) solution and *DT* to Dentz and Tartakovsky (2009a) solution.

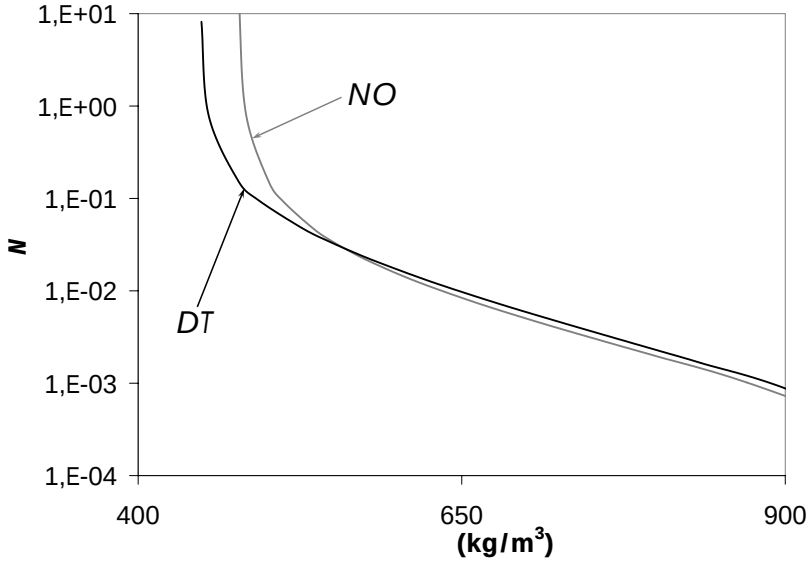

Fig. 8 Mean CO_2 density as a function of the gravity number in the cases discussed here for both analytical solutions. *NO* refers to Nordbotten et al (2005) solution and *DT* to Dentz and Tartakovsky (2009a) solution.